

Technical note

Application of spherical and cylindrical wrapping algorithms in a musculoskeletal model of the upper limb

Iain W. Charlton*, Garth R. Johnson

The Centre for Rehabilitation and Engineering Studies (CREST), Department of Mechanical, Materials and Manufacturing Engineering, Stephenson Building, University of Newcastle upon Tyne, Newcastle-upon-Tyne NE1 7RU, UK

Accepted 11 April 2001

Abstract

In the modelling of the upper limb, many muscles cannot be represented as a straight line from origin to insertion due to the complex morphology causing them to wrap around passive structures. The majority of bony contours that form these obstructions can be described adequately as simple geometric shapes such as spheres and cylinders.

A novel technique for the parameterisation of muscle paths as they wrap around such shapes has been developed for use in an upper limb model. The new method involves the definition of moving co-ordinate systems in which the path of a wrapped muscle does not move, allowing simplified specification. In addition, an analytical calculation of the wrapping path around a cylinder is presented over previous approximate methods.

Muscle moment arms were pre-calculated from vector considerations and within SIMM by tendon excursion. Close agreement between the two suggests that the proposed implementations accurately follow the theoretical relationship and can be used with confidence in musculoskeletal models. © 2001 Elsevier Science Ltd. All rights reserved.

Keywords: Muscle wrapping; Upper limb; Elbow; Pronation; Flexion

1. Introduction

In the static and dynamic modelling of musculoskeletal systems, one of the most important aspects is the calculation of muscle moment arms. These moment arms become constants in the equilibrium equations and hence are essential in the calculation of the resulting muscle and joint forces (An et al., 1984). The outcome of a model has been shown to be particularly sensitive to the musculotendon path when close to joint rotation centres (Winters and Stark, 1988).

Various methods have been utilised in the calculation of moment arms. An et al. (1981) used the centroid line of the muscle from serial cross sections in cadaveric experiments. Other cadaver experiments derive moment arms from tendon excursion (Franklin, 1994; Murray et al., 1995). More recently, 3-dimensional mathematical models are proving popular (Delp, 1990; Pronk, 1991; van der Helm, 1994), which predict the musculotendon

path from the model geometry. Muscles whose line of action is uninterrupted exert a force along the vector from origin to insertion and those affected by interfering structures exert forces at their origin, insertion and where they meet the offending structure at *effective* origins and insertions. The confidence with which models can be used is influenced not only by the quality of the morphometry data selected, but also by the presence of these effective origins and insertions.

2. Muscle wrapping path calculation

The earliest publication of a complete 3-dimensional geometry parameter set for the upper limb was by Hogfors et al. (1987) whose model included wrapping structures described in terms of simple cylinders, spheres and lines found from the study of three cadavers. Subsequent, more complete data sets have been published from the digitisation of bone surfaces and the least squares fitting of geometric shapes to them (van der Helm et al., 1992; Veeger et al., 1997) and those about

*Corresponding author. URL: www: <http://www.ncl.ac.uk/crest/>.

E-mail addresses: i.w.charlton@ncl.ac.uk (I.W. Charlton), g.r.johnson@ncl.ac.uk (G.R. Johnson).

which the muscles of the elbow wrap are summarised in Table 1. It is important to note that three of the muscles in question wrap around more than one structure.

The use of these parametric descriptions of wrapping structures requires the calculation of the shortest path from origin to insertion around the interfering structure, which follows the assumption that no friction or any other force acts between the muscle and bone surface.

The methods introduced here were developed for use in the Software for Interactive Musculoskeletal Modelling (SIMM, Musculographics Inc., IL, USA, Delp and Loan, 1995) which has since been upgraded to provide a facility for wrapping around simple structures. However, muscles may only wrap around one structure in SIMM, hence the methods presented here for wrapping path specification around more than one object are still of value when modelling with SIMM.

3. Spherical muscle wrapping

An analysis of spherical muscle wrapping has previously been conducted by van der Helm (1994) and analytical solutions can easily be found, locating effective origins (EO) and insertions (EI) on the sphere surface. In particular, the entire wrapping path is contained in the plane described by the origin, insertion and sphere centre, sometimes referred to as the dominant muscle plane (Runciman, 1993).

For generalised muscle wrapping, any rotation or translation of the wrapping structure affects the musculotendon path and the effects of these rotations and translations do not commute. Depending on the application, there are two ways in which this inseparable relationship can be resolved. Ideally, the positions of EI and EO should be determined at each instant and musculotendon length and moment arm calculated directly. Alternatively, a number of discrete points can be described and a piece-wise linear model used.

Musculotendon length can then be calculated as the sum of intermediate linear distances between points and hence moment arm derived as the (negative) rate of change of this length with respect to joint angle. The latter of these two methods is employed by SIMM and the path of wrapped muscles must be described in terms of a number of points fixed in a certain segment co-ordinate system. These individual wrapping sites can be made “active” over certain ranges of joint motion, hence allowing the wrapping path to change during the joint movement.

The description of the musculotendon line of action is simplified by defining an intermediate local co-ordinate system, $\{W\}$, centred at the sphere centre, \bar{C} , in which the tendon always passes through the $X-Y$ plane. This co-ordinate system is defined as follows:

$$\bar{X}_W = \frac{\overline{EO} - \bar{C}}{|\overline{EO} - \bar{C}|} \quad (1)$$

$$\bar{Z}_W = \frac{\overline{EO} \times \overline{EI}}{|\overline{EO} \times \overline{EI}|} \quad (2)$$

$$\bar{Y}_W = \bar{Z}_W \times \bar{X}_W. \quad (3)$$

The example illustrated in Fig. 1 shows this system, with the effective origin located at the top of the bicipital sulcus.

The relationship between this system and the segment embedded frame is described by a 4×4 transformation matrix, which, depending on the circumstances, may simplify. For the long head of biceps for example, the centre of the sphere describing the humeral head is coincident with both the glenohumeral joint rotation centre (van der Helm et al., 1989) and the origin of the humeral system (van der Helm, 1997). Thus, if we choose the sequence carefully, then only one Euler angle will be affected by humeral position, due to the effective origin being constrained by the bicipital sulcus (although this is not the general case).

Table 1
Passive wrapping structures in the upper limb

| Muscle | Wrapping structure | Approximate shape |
|---------------------|-----------------------------|-------------------|
| Biceps short | Capitulum and trochlea | Cylindrical |
| | Proximal radius | Cylindrical |
| Biceps long | Humeral head | Spherical |
| | Capitulum and trochlea | Cylindrical |
| Pronator teres | Proximal radius | Cylindrical |
| | Medial supracondylar ridge | Cylindrical |
| Triceps (all parts) | Capitulum and trochlea | Cylindrical |
| | Posterior humeral surface | — |
| Supinator | Olecranon | — |
| | Lateral supracondylar ridge | — |
| Anconeus | Proximal radius | Cylindrical |
| | Distal humerus | — |

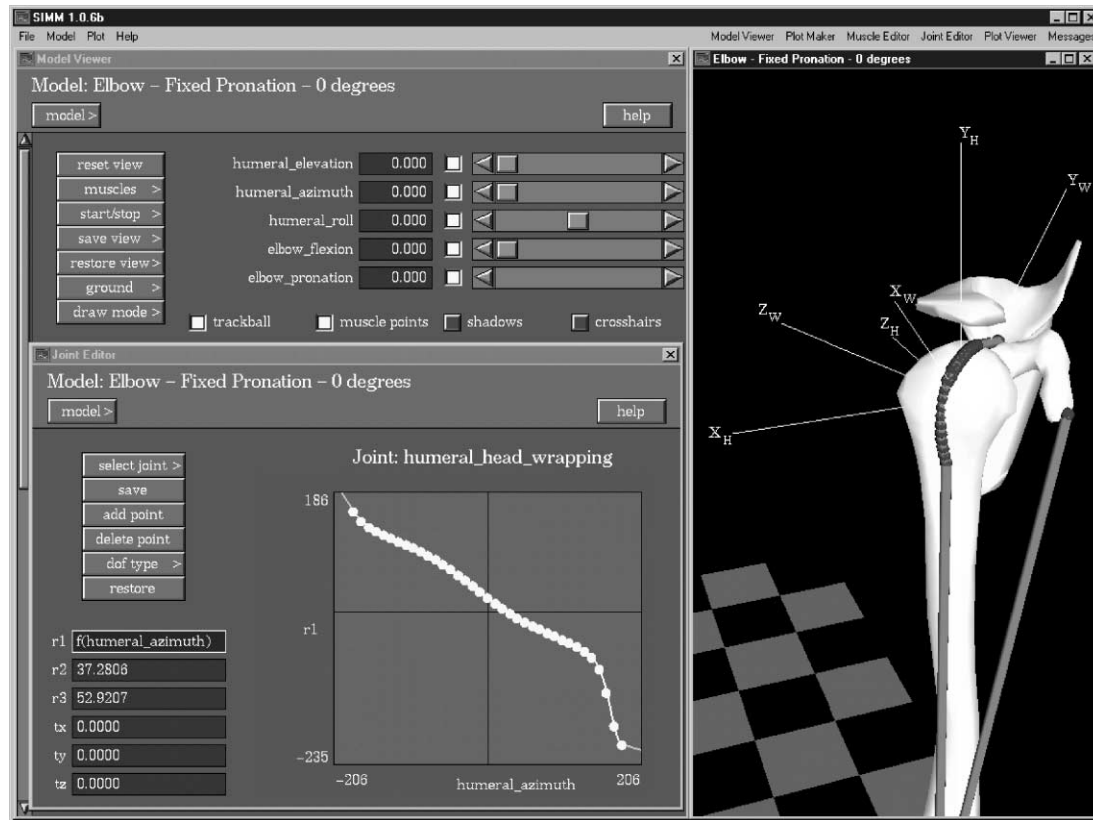


Fig. 1. Example of spherical muscle wrapping: SIMM implementation of long head of biceps wrapping around humeral head (for variable humeral azimuth only). Humeral and wrapping co-ordinate systems axes are shown and the Euler angles (sequence Z, Y', X''), with only the X'' rotation ($r1$ in the figure) dependent on humeral azimuth, which is specified at 5° intervals. Fixed muscle points within the bicipital sulcus are also shown.

This method of describing the wrapping path is advantageous, as the locations of the wrapping sites never change, only the number active. The technique can be used to specify a wrapping path based on either a single joint DOF, or alternatively time, where all joint angles (and displacements) are specified at each instant. Implementing this method involves defining the orientation of the intermediate system in terms of Euler angles and displacements, which are fixed or dependent on a joint angle (or time). Secondly, the maximum number of wrapping points possible are defined, determined by the desired resolution over the surface of the sphere, each being active over a certain range of the DOF being studied or period of time. The effect of more than one DOF can be simulated by employing a multi-dimensional look-up table of Euler angles (and displacements) with respect to the various joint DOF.

3.1. Spherical example: long head of biceps

The long head of biceps is constrained to a spherical path as it passes over the humeral head. A consideration of the location of the wrapping path depending purely

on humeral azimuth leads to the specification of two fixed Euler angles and one varying as shown in Fig. 1. This Figure also shows the orientation of the wrapping co-ordinate system in relation to the bones and the discrete wrapping points on the wrapping path.

4. Cylindrical muscle wrapping

It has previously been assumed (van der Helm, 1994) that the calculation of the shortest path around a cylinder must be an iterative process but that it can be approximated that the muscle lies entirely in one plane. In this paper, we present an analytical method for calculation of the path around a cylinder.

In order to find the location of the effective insertion, we must imagine the cylinder “unwrapped”, with this plane parallel with those containing the free portions of the muscle. The shortest path from origin to insertion in this configuration is hence a straight line as illustrated in Fig. 2.

This implies that the tendon wraps around the cylinder as a helix, that the tendon meets the cylinder

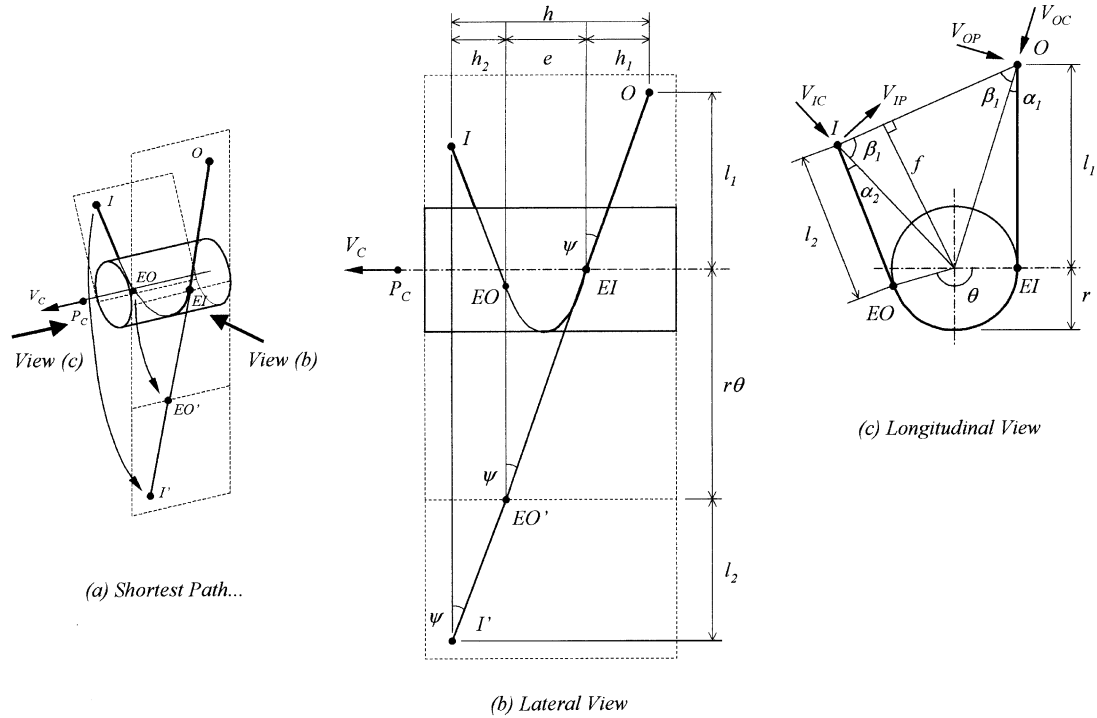


Fig. 2. Cylindrical muscle wrapping. (a) Shortest path from origin to insertion. (P_C and V_C are used to parametrise the cylinder and are the position and direction of V_C , respectively). (b) Lateral view (perpendicular to the plane containing O , EI and V_C). (c) Longitudinal view (along V_C).

as a tangent and that the orientation of the tendon is the same where it meets the cylinder as the free portions.

The mathematical interpretation of the three points forms a consideration of similar triangles, which yields

$$\frac{h_1}{l_1} = \frac{h_2}{l_2} = \frac{e}{r\theta} \quad (4)$$

therefore

$$h_1 = \frac{hl_1}{r\theta + l_1 + l_2} \quad (5)$$

and

$$h_2 = \frac{hl_2}{r\theta + l_1 + l_2}. \quad (6)$$

Thus, Eqs. (4) and (6) allow us to locate \overline{EI} and \overline{EO} through a knowledge of the distance shown in Fig. 4.

In order to determine these distances and angles, we must first define the following vectors, based on the locations of origin (\vec{O}), insertion (\vec{I}), a known arbitrary point on the cylinder axis (\vec{P}_C) and the cylinder axis itself (\vec{V}_C) as shown in Fig. 2:

$$\vec{V}_{OP} = \vec{V}_C \times \frac{(\vec{P}_C - \vec{O})}{|\vec{P}_C - \vec{O}|} \text{ and } \vec{V}_{IP} = \vec{V}_C \times \frac{(\vec{P}_C - \vec{I})}{|\vec{P}_C - \vec{I}|}, \quad (7)$$

$$\vec{V}_{OC} = \vec{V}_{OP} \times \vec{V}_C \text{ and } \vec{V}_{IC} = \vec{V}_{IP} \times \vec{V}_C. \quad (8)$$

Now, using these direction vectors and the cylinder axis, \vec{V}_C , we can easily calculate all of the lengths and angles shown in Fig. 2, allowing us to calculate the angle θ as follows:

$$\alpha_1 = \tan^{-1}\left(\frac{r}{l_1}\right) \text{ and } \alpha_2 = \tan^{-1}\left(\frac{r}{l_2}\right), \quad (9)$$

$$\beta_1 = \sin^{-1}\left(\frac{f}{l_1/\cos(\alpha_1)}\right) \text{ and } \beta_2 = \sin^{-1}\left(\frac{f}{l_2/\cos(\alpha_2)}\right). \quad (10)$$

Such that

$$\theta = -\alpha_1 + \beta_1 - \alpha_2 + \beta_2. \quad (11)$$

Knowledge of the distances h_1 and h_2 the angles α_1 , and α_2 , now allows us to locate \overline{EI} and \overline{EO}

$$\overline{EI} = \vec{O} + l_1 \cos(\alpha_1) \vec{V}_{OC} + l_1 \sin(\alpha_1) \vec{V}_{OP} + h_1 \vec{V}_C, \quad (12)$$

$$\overline{EO} = \vec{I} + l_2 \cos(\alpha_2) \vec{V}_{IC} - l_2 \sin(\alpha_2) \vec{V}_{IP} - h_2 \vec{V}_C. \quad (13)$$

Following the methodology developed for the spherical case, an intermediate co-ordinate system, $\{W\}$, is defined, in which the tendon follows a consistent path. Unfortunately, it is not generally possible to locate a helical locus in one single plane. This leads to the specification of a varying number of wrapping sites, which will move in relation to any intermediate frame $\{W\}$ we could specify. The discretised nature of these

attachment sites in SIMM can lead to errors in the calculation of musculotendon length and hence moment arm (see Discussion). For this reason, direct calculation of the effective origin and insertion, musculotendon length and hence, moment arm, is recommended where possible.

Despite these difficulties, a sensible choice of system is to align one of the $\{W\}$ axes with \bar{V}_C and to orient the second to pass through \bar{EI} or \bar{EO} . In the example shown in Fig. 3 for the biceps insertion on the radius, the system has been chosen such that \bar{EI} is fixed in this system and has zero \bar{Y}_W and \bar{Z}_W co-ordinates and a negative \bar{X}_W co-ordinate of r .

This system can be described as follows:

$$\bar{Y}_W = \bar{V}_C, \tag{14}$$

$$\bar{Z}_W = \bar{Y}_W \times \frac{(\bar{EI} - \bar{P}_C)}{|\bar{EI} - \bar{P}_C|}, \tag{15}$$

$$\bar{X}_W = \bar{Y}_W \times \bar{Z}_W. \tag{16}$$

Again, a finite number of sites must be chosen, based on some resolution criterion. If the cylinder axis is aligned with one of the segment embedded axes, then a single transformation can be implemented, with only one Euler rotation and one translation (along the cylinder axis) varying. If the cylinder axis is not aligned, then two transformations must be used, the first to align the first co-ordinate axes with the cylinder axis and the second to align the remaining axes.

5. Wrapping around multiple structures

Once algorithms for wrapping a musculotendon around simple shapes have been established, it is

relatively simple to extend the calculations to deal with more than one interfering structure.

The methods developed here do not analytically calculate a shortest path between origin and insertion, but iteratively find a path for which the assumptions for each of the individual wrapping algorithms are satisfied. The iterative process by which the stable path is found is summarised in Fig. 3.

The processes by which the effective origins and insertions are removed from within the respective structures are important for a well behaved, quick solution.

Other anatomical constraints can be built into these processes, in order to constrain the wrapping paths to certain “sides” of the cylinders and spheres. For example the biceps insertion wraps around both the distal humerus and the proximal radius, but it is constrained to wrap only around their anterior and medial surfaces, respectively.

Following this methodology, the inclusion of more structures is straightforward.

5.1. Multiple cylinders example: biceps

The biceps muscle wraps around many structures; the humeral head, distal humerus and proximal radius. Fig. 4 illustrates an implementation of the techniques described for wrapping around two cylinders. Both the long and short heads of the biceps muscle are shown, becoming unified in the common insertion tendon just superior to the capitulum.

The path of the biceps tendon is of course dependent on flexion and pronation and the combined effect could be studied using a 3D look up table of the variable Euler angle and displacement relating $\{W\}$ to $\{R\}$ with respect to both DOF.

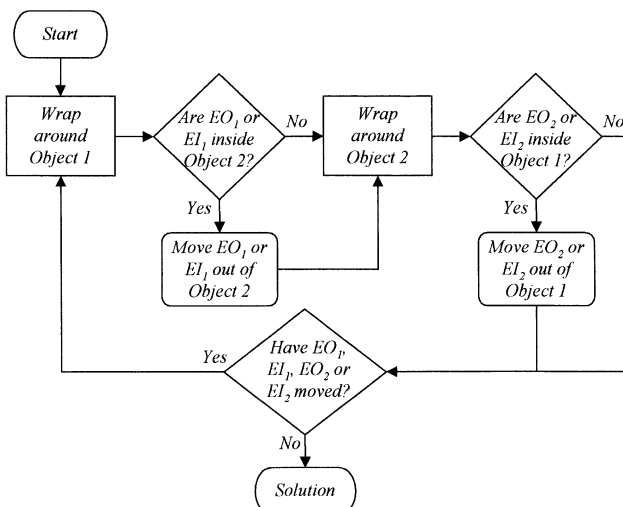
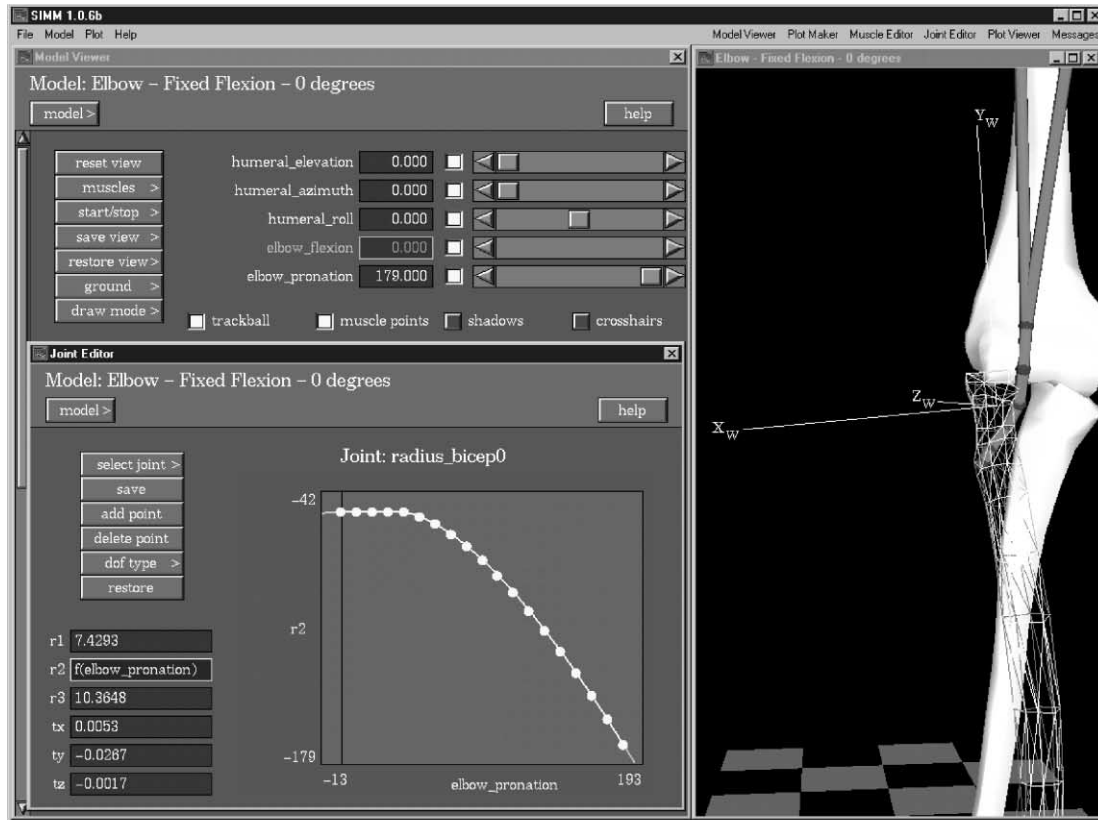


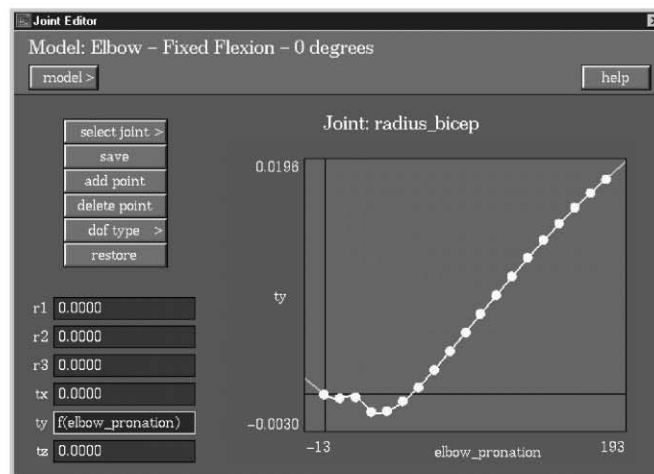
Fig. 3. Algorithm for wrapping around two structures.

6. Discussion

Within the context of musculoskeletal modelling, there are two possibilities for the calculation of muscle moment arms, from a vector consideration of the line of action or tendon excursion. Both of these methods are equally valid and can be divided only on grounds of computational efficiency or resolution specific to each modelling task. For the examples illustrated, moment arms were calculated directly during the derivation of the wrapping sites (as a perpendicular distance) and by tendon excursion within SIMM. The results shown in Fig. 5(b) and (c) are typical cross sections through the moment arm “surface” for a 90° flexed elbow and a 90° pronated forearm, respectively. No significant differences in correlation between the pre-calculated and SIMM moment arms were found for



(a)



(b)

Fig. 4. Example of multiple cylindrical muscle wrapping: SIMM implementation of biceps insertion wrapping around distal humerus and radius (for variable forearm pronation only). (a) The wrapping co-ordinate system axes are shown and the Euler angles (sequence Z, X', Y''), with only the Y'' rotation ($r2$ in the figure) dependent on forearm pronation, which is specified in 10° pronation intervals. The wrapping co-ordinate at the distal elbow is also shown. (b) The pronation dependent variable, displacement (ty in the figure) along the cylinder axis. This can be incorporated into the displacement along Y shown in (a), provided one to the body segment and cylinder axes are aligned.

other cross sections through the moment arm–flexion–pronation surface.

The errors in SIMM moment arms shown in Fig. 5(b) and (c) are due to instantaneous changes in musculo-tendon length (and hence moment arm) caused by the

discrete nature of the wrapping sites. Despite this, the SIMM results largely agree with the theoretical results *at the points of resolution* (i.e. at 5° intervals for the humeral head wrapping and 10° intervals for the elbow/radius wrapping).

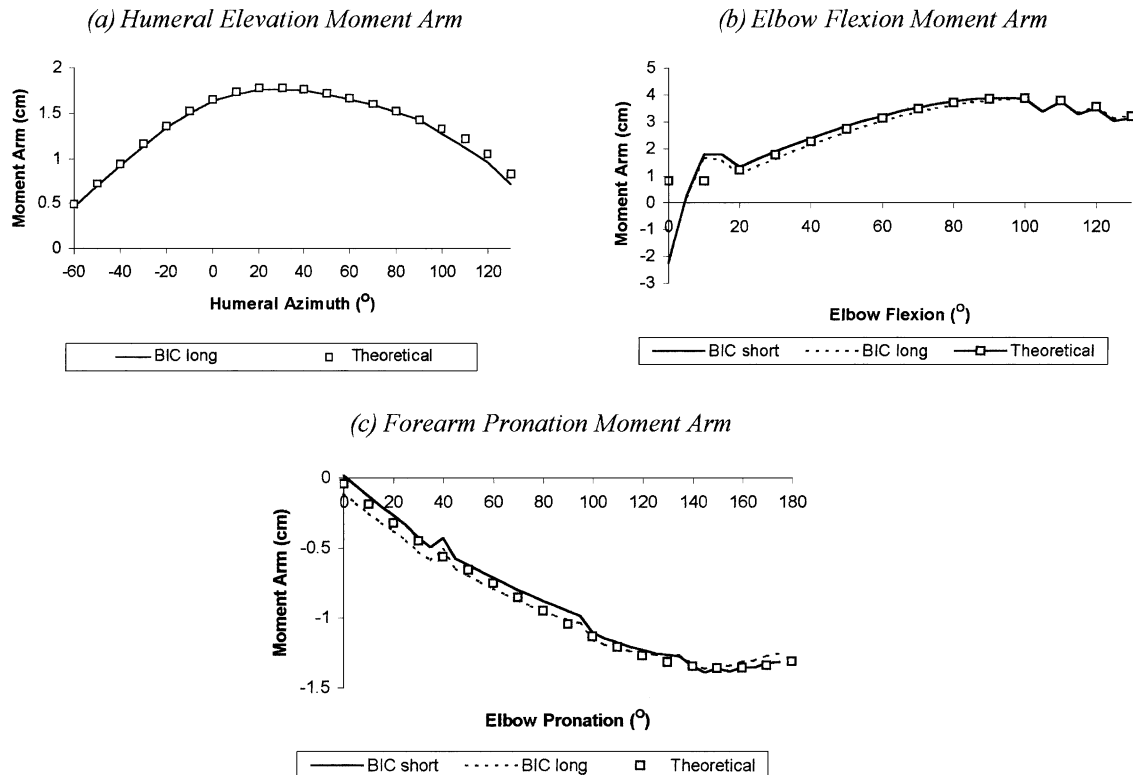


Fig. 5. Biceps moment arms. As calculated by SIMM and by theoretical consideration of musculotendon line of action. (a) Humeral head wrapping. (b) and (c) wrapping at the elbow and around the radius. (a) Humeral elevation moment arm. (b) Elbow flexion moment arm. (c) Forearm pronation moment arm.

It is also apparent from Fig. 5(a) that the spherical muscle wrapping technique is much more reliable than the cylindrical case due to the simple specification of a stationary wrapping path, minimising the magnitude of instantaneous change in musculotendon length.

The effect of discretisation of the wrapped muscle on the moment arm calculations can be minimised by using a greater resolution in both the specification of Euler angles with respect to joint DOF (i.e. using smaller angle intervals) and the discrete wrapping sites themselves. Computational constraints on the number and spatial resolution of wrapping sites will be specific to the system being modelled.

In conclusion, the wrapping algorithms presented here can be used with confidence for describing the wrapping of discretised musculotendon models. In particular, they can be used to extend SIMM's recently added wrapping facility to allow wrapping around more than one structure.

Acknowledgements

This work is part of a project funded by an EPSRC CASE award in conjunction with DePuy International Ltd.

References

- An, K.N., Hui, F.C., Morrey, B.F., Linscheid, R.L., Chao, E.Y., 1981. Muscles across the elbow joint: a biomechanical analysis. *Journal of Biomechanics* 14, 659–669.
- An, K.N., Takahashi, K., Harrigan, T.P., Chao, E.Y., 1984. Determination of muscle orientation and moment arms. *Journal of Biomechanical Engineering* 106, 280–282.
- Delp, S.L. (1990) Surgery simulation: a computer graphics system to design and analyze musculoskeletal reconstructions of the lower limb. Ph.D. Thesis, Stanford University.
- Delp, S.L., Loan, J.P., 1995. A graphics-based software system to develop and analyze models of musculoskeletal structures. *Computers in Biology and Medicine* 25, 21–24.
- Franklin, P. (1994) Functional anatomy of the glenohumeral joint. Ph.D. Thesis, University of Strathclyde, Glasgow.
- Murray, W.M., Delp, S.L., Buchanan, T.S., 1995. Variation of muscle moment arms with elbow and forearm position. *Journal of Biomechanics* 28, 513–525.
- Pronk, G.M., 1991. The shoulder girdle: analysed and modelled kinematically. Ph.D. Thesis, Delft University of Technology, Delft.
- Runciman, R.J., 1993. Biomechanical model of the shoulder joint. Ph.D. Thesis, University of Strathclyde, Glasgow.
- van der Helm, F.C.T., 1994. A finite element musculoskeletal model of the shoulder mechanism. *Journal of Biomechanics* 27, 551–569.
- Van der Helm, F.C.T., 1997. A standardised protocol for motion recordings of the shoulder. In: Veeger, H.E.J., van der Helm, F.C.T., Rozing, P.M. (Eds.) *First Conference of the International Shoulder Group* (Edited by Ssaker Publishers, Maastricht, Delft. pp. 47–51.

- van der Helm, F.C.T., Pronk, G.M., Veeger, H.E.J., Van der Woude, L.H.V., 1989. The rotation centre of the glenohumeral joint. XII International Congress of Biomechanics, Los Angeles, USA.
- van der Helm, F.C.T., Veeger, H.E.J., Pronk, G.M., Van der Woude, L.H.V., Rozendaal, R.H., 1992. Geometry parameters for musculoskeletal modelling of the shoulder mechanism. *Journal of Biomechanics* 25, 129–144.
- Veeger, H.E.J., Yu, B., An, K.N., Rozendal, R.H., 1997. Parameters for modeling the upper extremity. *Journal of Biomechanics* 30, 647–652.
- Winters, J.M., Stark, L., 1988. Estimated mechanical properties of synergistic muscles involved in movements of a variety of human joints. *Journal of Biomechanics* 21, 1027–1041.